Distinct Roles of Two Mg^{2+} Binding Sites in Regulation of Murine Flap Endonuclease-1 Activities†

Li Zheng,‡ Mei Li,‡ Jixiu Shan,§ Ramaswamy Krishnamoorthi,§ and Binghui Shen*,‡

Division of Molecular Medicine, City of Hope National Medical Center and Beckman Research Institute, Duarte, California 91010, and Department of Biochemistry, Kansas State University, Manhattan, Kansas 66506

Received March 20, 2002; Revised Manuscript Received June 18, 2002

ABSTRACT: Removal of flap DNA intermediates in DNA replication and repair by flap endonuclease-1 (FEN-1) is essential for mammalian genome integrity. Divalent metal ions, Mg^{2+} or Mn^{2+}, are required for the active center of FEN-1 nucleases. However, it remains unclear as to how Mg^{2+} stimulates enzymatic activity. In the present study, we systemically characterize the interaction between Mg^{2+} and murine FEN-1 (mFEN-1). We demonstrate that Mg^{2+} stimulates mFEN-1 activity at physiological levels but inhibits the activity at concentrations higher than 20 mM. Our data suggest that mFEN-1 exists as a metalloenzyme in physiological conditions and that each enzyme molecule binds two Mg^{2+} ions. Binding of Mg^{2+} to the M1 binding site coordinated by the D86 residue cluster enhances mFEN-1's capability of substrate binding, while binding of the metal to the M2 binding site coordinated by the D181 residue cluster induces conformational changes. Both of these steps are needed for catalysis. Weak, nonspecific Mg^{2+} binding is likely responsible for the enzyme inhibition at high concentrations of the cation. Taken together, our results suggest distinct roles for two Mg^{2+} binding sites in the regulation of mFEN-1 nuclease activities in a mode different from the "two-metal mechanism".

Murine flap endonuclease-1 (mFEN-1) was first isolated by Harrington and Lieber when searching for structure-specific nucleases for processing of recombinational intermediates for generation of antibody diversity (*1*). Work from several other groups has indicated that mammalian FEN-1[1] nucleases possess flap endonuclease activity as well as 5′ nick-specific exonuclease activity (*1*−*5*). These nuclease activities allow FEN-1 proteins to remove RNA primers during lagging-strand DNA synthesis and DNA lesion fragments in various DNA repair pathways (*6*−*11*). The nuclease interacts with various proteins involved in DNA metabolic pathways, including the Werner syndrome protein (WRN; *12*) and proliferating cell nuclear antigen (PCNA; *13*, *14*). FEN-1 localizes to the nucleus during DNA synthesis and in response to DNA damage (*15*). In yeast, loss of FEN-1 functions was determined to cause severely impaired phenotypes, including conditional lethality, a dramatic increase of cellular sensitivity to alkylating agents, e.g., methyl methanesulfonate (MMS), and a significant increase in the mutation rate. Interestingly, the majority of mutations in the yeast null mutant strains are large sequence duplications (*10*), which in humans have been associated with genetic diseases including cancers. FEN-1 is also a key enzyme involved in preventing expansion and contraction of bi- or trinucleotide repeats (*16*−*19*). More recently, we have demonstrated that FEN-1 nucleases played a major role in limiting short sequence recombination for yeast genome stability (*20*).

Bambara and colleagues proposed a "thread-through model" to explain the molecular mechanism of the structure-specific nucleases. In this model, FEN-1 specifically recognizes the 5′-phosphate group on the single-strand DNA, migrates down the flap arm, and then cleaves the substrate at the junction of single- and double-stranded DNA (*21*, *22*). Multiple amino acid sequence analysis of FEN-1s from different species reveals that the enzyme contains two conserved nuclease motifs, the N and I domains, at the N-terminus (*4*, *23*, *24*). The crystal structures of FEN-1 homologues, including T5 exonuclease and archaebacterial FEN-1 (aFEN-1), indicate that the N domain, I domain, and the loop region linking these two motifs form a hole structure (*25*−*27*). The dimension of the hole in the middle of the protein allows only single-stranded DNA to thread through. Furthermore, the H3TH motif, two antiparallel β-sheets, and a region that contains R47 and R70 in human FEN-1 (hFEN-1) have been identified as critical for the enzyme to bind the flap DNA substrate and hold the substrate in the most efficient orientation to facilitate the cleavage (*28*). Seven to eight conserved acidic amino acid residues and two divalent metal ions, either Mg^{2+} or Mn^{2+}, have been identified in the nuclease motifs from different homologues of FEN-1 enzymes via amino acid sequence comparison and crystal structural analysis (*29*). These residues were determined to be critical for metal coordination and formation of an active center, as individual mutation of these residues resulted in

†This work was supported by National Institutes of Health Grant CA73764 (to B.S.).

* To whom correspondence should be addressed. Tel: (626) 301-8879. Fax: (626) 301-8972. E-mail: bshen@coh.org.

‡ City of Hope National Medical Center and Beckman Research Institute.

§ Kansas State University.

[1] Abbreviations: FEN-1, flap endonuclease-1; DNA, deoxyribonucleic acid; SDS, sodium dodecyl sulfate; PAGE, polyacrylamide gel electrophoresis; DTT, dithiothreitol; ITC, isothermal titration calorimetry; CD, circular dichroism.

10.1021/bi025841s CCC: $22.00
Published on Web 07/19/2002

loss of cleavage activities (*23*, *30*, *31*).

Magnesium, the most abundant divalent metal ion in mammalian cells, plays structural and catalytic roles in many cellular processes that affect genome stability (*32*). Mg^{2+} functions as a cofactor of proteins involved in DNA replication and repair pathways. It is required for activity and fidelity of DNA polymerases (*33*). It is also required for the activities of nucleases, such as for AP endonuclease (*34*, *35*) and MutH (*36*) nucleases, which are involved in many DNA repair pathways, including nucleotide excision repair (NER), base excision repair (BER), and DNA mismatch repair (MMR). Two models, "one-metal mechanism" and "two-metal mechanism", were proposed to explain roles of Mg^{2+} in nucleases. In the one-metal mechanism model, on the basis of studies with *Escherichia coli* RNase H (*37*) and AP endonuclease (*34*), a single Mg^{2+} binds to the enzymes, orients the phosphate group of the P−O3′ bond, and assists the attack on this bond. Alternatively, the two-metal mechanism model was proposed on the basis of studies with the 3′ nuclease domain of *E. coli* DNA polymerase I (*38*). In these enzymes, the first metal ion activates a water molecule to attack the P−O3′ bond, while the second metal ion helps to maintain a phosphorane intermediate. Both metal ions are required to stabilize the substrate−enzyme complex.

According to the crystal structure of aFEN-1 (*26*) and mutagenic analysis of aFEN-1 and hFEN-1 (*23*, *26*), two Mg^{2+} have been observed in the active center of FEN-1. Under the two-metal mechanism model, chemical transitions of diphosphate bond breakage require the two metal ions in the active center to be close with a maximal distance of 2 Å. However, the metal ions bound to FEN-1 are approximately 5 Å apart (*26*). Previous studies also showed that binding of Mg^{2+} induced conformational changes (*39*, *40*), which may be important for catalysis. To study the role of metal ions in the FEN-1-catalyzed chemical transition, we carried out a series of biochemical and biophysical experiments and characterized Mg^{2+} effects on protein conformation, substrate binding, and enzyme activities of recombinant wild-type mFEN-1 and various active center mutants with defects in Mg^{2+} binding. We found that Mg^{2+} modulated mFEN-1 activities in a dose-dependent manner and that millimolar ranges of Mg^{2+} were required for optimal nuclease activities. However, Mg^{2+} inhibits the enzymatic activity at concentrations above 20 mM. Our data also revealed that two Mg^{2+} ions are synergistically incorporated into the active center of mFEN-1. The biochemical roles of these two metal ions are distinct. Binding of Mg^{2+} to the M1 binding site of mFEN-1 facilitates the enzyme to recruit substrates, while binding of the metal ion to the M2 binding site triggers conformational changes. Both metal ions are required for enzymatic activity. In the presence of higher concentrations of Mg^{2+}, such as 50 mM, the metal ion inhibits mFEN-1, very likely by nonspecific binding or by general electrostatic effects.

MATERIALS AND METHODS

Construction of the Overexpression Plasmids of 6His-Tagged mFEN-1 and Its Mutants. A DNA fragment encoding mFEN-1 was generated by the polymerase chain reaction (PCR) using the BAC-FEN-1 plasmid (Genomesystems, Inc., St. Louis, MO) as the template and two synthetic oligonucleotides as 5′ and 3′ primers, which include a *Nco*I and a *Hin*dIII restriction site at their 5′ ends, respectively. There is no intron in the open reading frame (ORF) of mFEN-1. The PCR-amplified fragment was digested with *Nco*I and *Hin*dIII restriction enzymes (New England Biolabs, Beverly, MA) and ligated directly into the pET-28b plasmid (Novagen, Madison, WI). The constructs encoding mutant mFEN-1 proteins in this study were created using the QuickChange site-directed mutagenesis kit (Stratagene, La Jolla, CA). The primers used for preparation of wild-type and mutant mFEN-1 were designed and listed in Table 1. The constructs were verified by DNA sequencing (DNA Sequencing Facility, City of Hope) and transformed into *E. coli* strain BL21-(DE3) for protein expression.

Table 1: Oligonucleotides Used in This Study for Amplification of the mFEN-1 Open Reading Frame and Construction of mFEN-1 Mutants

mFEN-1	oligos	oligo sequence
wild type	mFEN-1F	5′-CTACCATGGGAATTCACGGCCTTGCC-3′
	mFEN-1R	5′-GCCCAAGCTTAGTGATGATGATGATG-ATGTTTTCCCCTTCGGAACTTCCCCGC-3′
D86A	D86A-F	5′-CTGTGTACGTCTTT**gc**TGGCAAACCACC-3′
	D86A-R	5′-GGTGGTTTGCCA**gc**AAAGACGTACACAG-3′
D181A	D181A-F	5′-CGGAGGACATG**gc**CTGCCTCACTTTTG-3′
	D181A-R	5′-CAAAAGTGAGGCAG**gc**CATGTCCTCCG-3′

Protein Expression and Purification of Metal-Free mFEN-1 and the Mutant Proteins. The *E. coli* BL21(DE3) cells that harbor the plasmid encoding His-tagged mFEN-1 or its mutants were grown at 37 °C to an absorbance of about 1.0 at 600 nm and induced by 1 mM isopropyl thio-β-galactopyranoside (IPTG) for 4 h. Cells were harvested and lysed by sonication. The soluble His-tagged fusion proteins were purified by a fast protein liquid chromatography (FPLC; Pharmacia Biotech, Piscataway, NJ) system with a Ni^{2+} chelating column, according to a previously described protocol (*41*). The purified fusion proteins were extensively dialyzed against a Chelex-100 (Sigma, St. Louis, MO) treated buffer, containing 20 mM Tris-HCl, pH 7.5, and 150 mM NaCl, to remove trace amounts of metal. The proteins were then concentrated using Centricon concentrators (Millipore, Bedford, MA). Protein concentration was determined using the ϵ_{280} value of 21260 M^{-1} cm^{-1} and the molecular mass of 42314 Da, calculated by the GCG program (University of Wisconsin, Madison, WI) on the basis of the amino acid sequence of mFEN-1. The mutant proteins have similar ϵ_{280} and molecular mass values according to the calculation. The purified fusion proteins were verified to be free of metal ions using inductive coupled plasma (ICP) analysis (Quantitative Technologies Inc., Whitehouse, NJ). The purified metal ion-free mFEN-1 and the mutants were either used immediately or stored at −20 °C after addition of an equal volume of glycerol. The solutions used for protein purification and other experiments were prepared using Chelex-100 treated deionized water to remove trace amounts of divalent metal ions.

Preparation of DNA Substrate for Nuclease Activity and DNA Substrate Binding Assays. The 5′ flap DNA substrate was prepared according to a published procedure (*41*). Three synthetic oligonucleotides were used: Flap-G1 (5′-GATGTCAAGCAGTCCTAACTTTGAGGCAGAGTCC-3′), Exo-3PT (5′-TTGAGGCAGAGTCC-3′), Temp-1G (5′-GGACTCTGCCTCAAGACGGTAGTCAACGTG-3′), and Prim-3B (5′-

CACGTTGACTACCGTC-3′). To label DNA substrates, 80 pmol of Flap-G1 or Exo-3PT, which is for flap-specific or nick-specific DNA substrate, respectively, was incubated with 20 μCi of [γ-^{32}P]ATP and 10 units of polynucleotide kinase at 37 °C for 30 min. After inactivation of polynucleotide kinase by heating the sample at 72 °C, 160 pmol each of Temp-1G and Prim-3B was added to the reaction. The samples were incubated at 70 °C for 5 min and slowly cooled to 30 °C to allow the formation of substrates. They were precipitated by addition of 20 μL of 3 M NaOAc and 1 mL of absolute ethanol and resuspended in water. For the DNA binding assay, the 5′ biotinylated Temp-1G was annealed with unlabeled Flap-G1 and Prim-3B using the same annealing protocol.

Divalent Metal Ion-Dependent Nuclease Activities of mFEN-1. The nuclease activity was assayed following a modified version of the previously described method (*41*) to test the effect of metal ions on enzyme catalytic capacity. Two picomoles of mFEN-1 or its mutant proteins was incubated with 500 fmol of flap or nick substrate in 15 μL of reaction buffer (50 mM Tris-HCl, pH 8.0) containing no Mg^{2+} or various concentrations of the metal ion. To determine the effect of different metal ions, 1 mM Ca^{2+}, Co^{2+}, Cu^{2+}, Mg^{2+}, Mn^{2+}, Ni^{2+}, or Zn^{2+} was included in the reaction. The reaction was incubated at 30 °C for 15 min and terminated by addition of an equal volume of stop solution (95% formamide, 20 mM EDTA, 0.05% bromophenol blue, 0.05% xylene cyanol). The product and substrate were then separated by 15% denaturing polyacrylamide gel electrophoresis (PAGE) and visualized by autoradiography.

Microcalorimetric Titration of mFEN-1 by Mn^{2+}. Thermodynamic properties of metal binding by mFEN-1 were explored by isothermal titration calorimetry (ITC) using a MicroCal OMEGA calorimeter (*42*). Wild-type mFEN-1, D86A, or D181A resuspended in a Chelex-100 treated buffer containing 50 mM Tris-HCl (pH 7.5) and 200 mM NaCl was placed in a 1.38 mL sample cell. A syringe (250 μL) loaded with 2 mM standard $MnCl_2$ solution (Fisher Scientific, Tustin, CA) was used for a series of automatic injections of 10 μL each into a protein solution. Heat produced due to dilution was measured by injecting the Mn^{2+} solution into the same buffered solution excluding mFEN-1. For each titration step, the heat of dilution was subtracted from the corresponding Mn^{2+} binding data of mFEN-1. Data were fit to appropriate binding models and thermodynamic parameters determined from nonlinear least-squares fits, using the ORIGIN software (MicroCal, Northampton, MA).

Determination of Stoichiometry of Mg^{2+} Binding. Mg^{2+} binding by mFEN-1 and its mutants was evaluated by ultrafiltration using Centrifree centrifugal filter devices (Millipore, Bedford, MA; *43*). Certain amounts of Mg^{2+}-free wild-type mFEN-1, D86A, or D181A, ranging from 100 to 500 μM, were saturated with 2 mM Mg^{2+} at 4 °C for 30 min. Protein solution was then transferred to a Centrifree centrifugal filter device with a molecular mass cutoff value of 30000 kDa and centrifuged at 1000*g* for 90 s at 4 °C. To ensure that no Mg^{2+} ion was retained by the filter membrane, a control experiment was performed under the same condition on a buffer solution without protein. The Mg^{2+} concentrations of the original solution and the filtrated solution were determined by a modified version of calmagite colorimetric measurement (*44*). Briefly, 10 μL of standard Mg^{2+} solution or sample was mixed with 990 μL of freshly made 50 mM Tris-HCl, pH 10, containing 0.005% calmagite solution (Sigma, St. Louis, MO). After the solution was allowed to stand for 5 min, its absorbance at 520 nm was determined against the blank with a Ultrospec 3000 UV/visible spectrometer (Pharmacia Biotech, Piscataway, NJ). The Mg^{2+} concentration of each sample was independently measured three times. Mg^{2+} bound to the protein was determined by subtracting the free Mg^{2+} concentration of the filtrated solution from that of the original solution. The number of metals binding by mFEN-1 or the mutants was calculated on the basis of the amount of Mg^{2+} ion bound to the protein and the protein concentration. The ultrafiltration assay for each protein sample was performed three times. The stoichiometry value represented the average of three experiments.

DNA Substrate Binding Assay. The DNA substrate binding ability was measured using a similar method as published previously (*45*). The biotinylated DNA substrate was immobilized onto the Neutro-avidin agarose by incubation in 10 mM Tris-HCl, pH 7.5, 1 mM EDTA, and 1 M NaCl at 25 °C for 2 h. The beads were washed twice with the same buffer solution used for the linking reaction and resuspended in a solution containing 30 mM Hepes−NaOH, pH 7.5, 125 mM NaCl, 0.2 mg/mL BSA, and 1 mM dithiothreitol (DTT). DNA-bound beads were incubated with 5 pmol of FEN-1 proteins in the presence of 0, 5, 20, or 50 mM Mg^{2+} on ice for 1 h. The beads were then washed twice with a buffered solution (30 mM Hepes−NaOH, pH 7.5, 125 mM NaCl, 0.1 mg/mL BSA, 5% glycerol, 1 mM DTT, 0.01% NP-40, and a corresponding amount of Mg^{2+} ion). The beads were boiled in 2× protein sample buffer (100 mM Tris-HCl, pH 6.8, 200 mM DTT, 4% SDS, 0.2% bromophenol blue, and 20% glycerol). The protein supernatant was collected and separated by 10% sodium dodecyl sulfate−polyacrylamide gel electrophoresis (SDS−PAGE). The proteins were detected by immunoblot using monoclonal anti-FEN-1 antibody (Santa Cruz Biotechnology, Santa Cruz, CA) as the first antibody and visualized using a supersignal pico chemiluminescence substrate (Pierce, Rockford, IL).

Trypsin Sensitivity Assay of FEN-1 Proteins. The limited trypsin cleavage of mFEN-1 and mutants was carried out at 25 °C, according to a previously published procedure (*46*). Purified FEN-1 proteins were incubated with sequence grade trypsin (Promega, Madison, WI) at a ratio of 1000:1 in a buffer solution (25 mM Tris-HCl, pH 8.0, 150 mM NaCl) containing various concentrations of Mg^{2+} (0, 0.01, 0.1,1, 5, 10, 20, or 50 mM). After 1 h incubation, the reaction was terminated by addition of the protein sample buffer (100 mM Tris-HCl, pH 6.8, 200 mM dithiothreitol, 4% SDS, 0.2% bromophenol blue, and 20% glycerol). The mixture was then boiled for 5 min, and an aliquot of each reaction mixture was then analyzed by a 4%−20% gradient gel (Bio-Rad, Hercules, CA).

RESULTS

Activation of FEN-1 by Divalent Metal Ions. Mg^{2+} or Mn^{2+} is required for both flap endonuclease and exonuclease activity of FEN-1 (*1*). Other divalent metal ions, Ca^{2+}, Co^{2+}, Cu^{2+}, Ni^{2+}, and Zn^{2+}, were tested for their abilities to activate the enzymatic activity. Our results confirm that Mg^{2+} and Mn^{2+} show maximum stimulation of mFEN-1 and that Co^{2+}

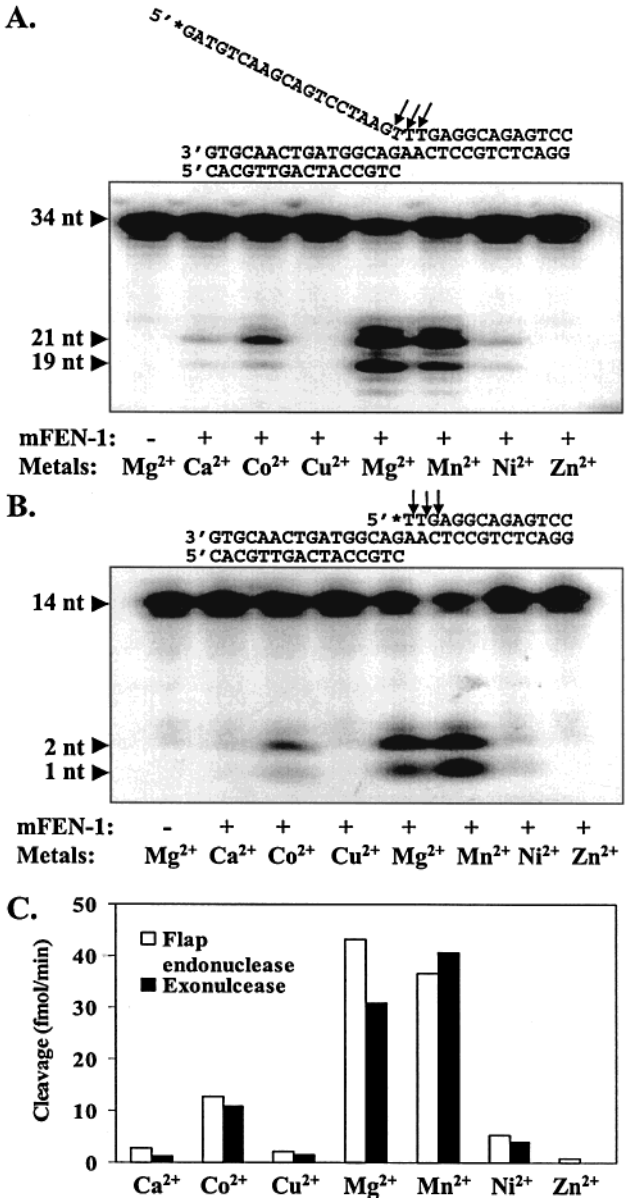

FIGURE 1: Divalent metal ion dependence of mFEN-1 nuclease activities. The flap-specific endonuclease and nick-specific exonuclease activities of purified recombinant mFEN-1 were assayed in the presence of different divalent ions. Lanes 2−8 represent Ca^{2+}, Co^{2+}, Cu^{2+}, Mg^{2+}, Mn^{2+}, Ni^{2+}, and Zn^{2+}, respectively. The reactions were carried out by incubation of 2 pmol of purified mFEN-1 and 1 pmol of ^{32}P-labeled flap endo-DNA or nick exo-DNA substrate suspended in 50 mM Tris-HCl (pH 8.0) buffer with 1 mM indicated metal ion. After incubation at 30 °C for 15 min, the reactions were terminated by addition of an equal volume of stop solution (95% formamide, 20 mM EDTA, 0.05% bromophenol blue, 0.05% xylene cyanol). The substrates and products were resolved in a 15% denaturing PAGE and visualized by autoradiography. 34 nt and 14 nt are the labeled oligos in flap endo and exo substrates, respectively, as pictorially presented on the top of each gel image. 21 nt, 19 nt, 2 nt, and 1 nt are the cleaved products of the endo- and exonucleases of mFEN-1. (A) Pictorial representation of flap endonuclease acitivity. (B) Representation of nick exonuclease activity. (C) Nuclease activities quantified by the IPLab Gel program (Signal Analytics Corp., Vienna, VA).

also has a considerable activation effect. Ca^{2+} and Ni^{2+} exhibit a very weak stimulation of mFEN-1, while Cu^{2+} and Zn^{2+} do not stimulate the enzymatic activity of mFEN-1 (Figure 1). The Mg^{2+} concentration dependency of the nuclease activity of mFEN-1 was determined. The results

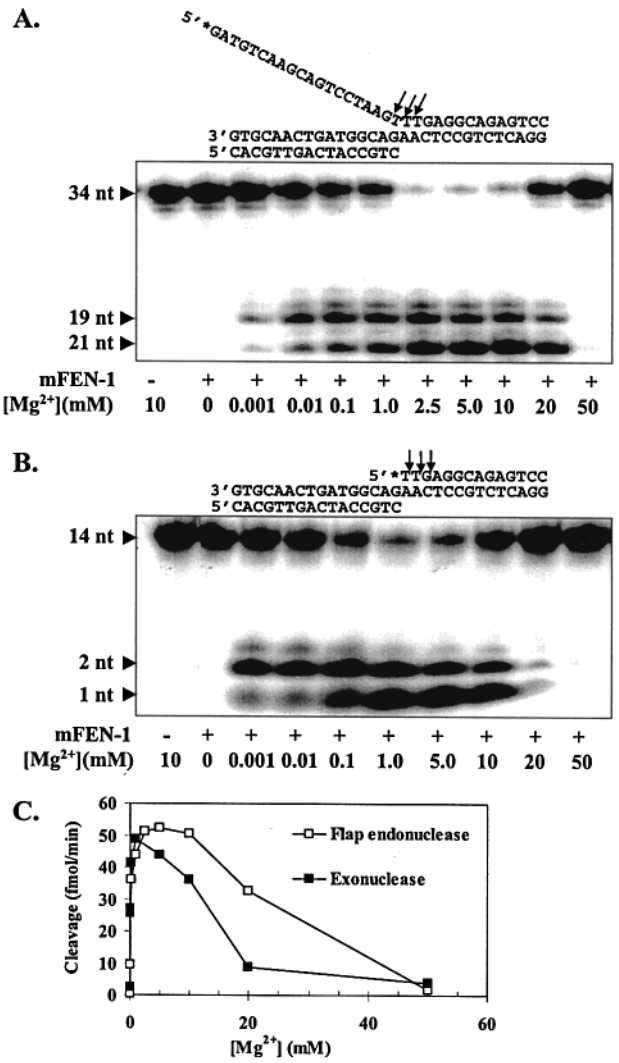

FIGURE 2: Mg^{2+} concentration dependence of Flap endo- and exonuclease activities of mFEN-1. 2 pmol of purified mFEN-1 was incubated at 30 °C for 15 min with 1 pmol of ^{32}P-labeled flap endo-DNA or nick exo-DNA substrate in a buffered solution containing 50 mM Tris-HCl (pH 8.0) and various concentrations of Mg^{2+} ion. The cleavage efficiency was analyzed by 15% denaturing PAGE and autoradiography. (A) Flap endonuclease activity. Lane 1 is the background hydrolysis of flap DNA substrate in the absence of mFEN-1. Lanes 2−11 represent the cleavage of flap DNA substrate by mFEN-1 in the presence of 0.001, 0.01, 0.1, 1, 2.5, 5, 10, 20, and 50 mM Mg^{2+}. (B) Exonuclease activity assays. Lane 1 is the background hydrolysis of nick DNA substrate in the absence of mFEN-1. Lanes 2−10 represent the cleavage of nick DNA substrate by mFEN-1 in the presence of 0.001, 0.01, 0.1, 1, 5, 10, 20, and 50 mM Mg^{2+}. (C) Mg^{2+} dose-dependent nuclease activities quantified by the IPLab Gel program.

indicate that both flap endonuclease and exonuclease activities of mFEN-1 are stimulated by low concentrations of Mg^{2+} in a dose-dependent manner but are inhibited by high concentrations of the cation. Optimal flap endo- and exonuclease activities occur in the presence of 5 and 1 mM Mg^{2+}, respectively (Figure 2). Enzyme activities are completely suppressed when the metal ion concentration reaches 50 mM (Figure 2).

Kinetics Analysis of mFEN-1 as a Function of Mg^{2+} Concentration. To explore the mechanism by which Mg^{2+} stimulates mFEN-1 at low concentrations but inhibits the enzyme at high concentrations, kinetic parameters were determined for DNA substrate catalysis by mFEN-1 in the

Table 2: Kinetic Parameters of Nuclease Activities of mFEN-1

flap endonuclease activity				exonuclease activity			
$[Mg^{2+}]$ (mM)	k_{cat} ($\times 10^{-2}$/ min)	K_m (nM)	k_{cat}/K_m [$\times 10^{-4}$/ (nM·min)]	$[Mg^{2+}]$ (mM)	k_{cat} ($\times 10^{-2}$/ min)	K_m (nM)	k_{cat}/K_m [$\times 10^{-4}$/ (nM·min)]
0.01	9.0	89.3	10.1	0.01	2.0	295.2	0.7
5	15.0	36.9	43.1	1	8.2	158.6	5.0
20	11.9	90.2	13.2	20	0.9	513.8	0.2

presence of different Mg^{2+} concentrations. Three concentrations of Mg^{2+} were chosen for conventional steady-state kinetic study: low level (0.01 mM), optimal level (5 mM for flap endonuclease and 1 mM for exonuclease), and inhibitory level (20 mM). The Michaelis−Menten kinetic analysis was used to derive K_m, k_{cat}, and k_{cat}/K_m values, which are summarized in Table 2. Compared with the k_{cat} and K_m values at optimal Mg^{2+} concentration, the k_{cat} at 0.01 mM Mg^{2+} decreases 40% or 76% for endo- or exonuclease, respectively, and the K_m increases 2.4-fold or 1.9-fold for endo- or exonuclease, correspondingly. Similarly, for flap endonuclease activity, the k_{cat} at 20 mM Mg^{2+} decreases about 21% and the K_m increases 2.4-fold. For exonuclease activity, the k_{cat} at 20 mM Mg^{2+} decreases about 89% and the K_m increases 3.2-fold. The rate constant k_{cat}/K_m of mFEN-1 at 0.01 mM Mg^{2+} decreases about 4-fold or 7-fold for flap endo- or exonuclease activity, respectively, compared with those at optimal Mg^{2+} concentration. Likewise, k_{cat}/K_m at 20 mM Mg^{2+} decreases 3.3-fold or 25-fold for flap endo- or exonuclease activity, correspondingly. At high concentration (20 mM), Mg^{2+} affects k_{cat}/K_m of exonuclease much more than that of flap endonuclease.

Different Concentrations of Mg^{2+} Change the Trypsin Digestion Pattern of mFEN-1 Due to Conformational Changes. Previous studies on hFEN-1 nuclease showed that binding of Mg^{2+} could lead to conformational changes of the protein (*39*, *40*). According to our kinetic data, we further suggest that in the absence of Mg^{2+} mFEN-1 is in an inactive conformation, while at optimal concentrations of Mg^{2+} the enzyme is triggered into an active conformation. However, at Mg^{2+} concentrations above optimal, mFEN-1 is converted to a different inactive conformation. To test this hypothesis, the trypsin sensitivity assay was employed to monitor conformational changes upon binding of Mg^{2+} (Figure 3). Digestion of mFEN-1 by trypsin results in accumulation of three clear bands, A, B, and C, within molecular mass ranges of 25−42 kDa and several other lower molecular mass bands that overlap each other. To compare the trypsin digestion pattern in various Mg^{2+} levels, bands A, B, and C were picked up for semiquantification. The ratio of intensity of each band over the intensity of total noncleaved mFEN-1 was calculated. In the absence of Mg^{2+}, digestion of mFEN-1 leads to accumulation of 26% band B, 34% band C, and only 2% band A with respect to total protein input (Figure 3). However, in the presence of Mg^{2+} as low as micromolar levels (Figure 3), there is an increase in accumulation of band A but a decrease in amounts of bands B and C. The decrease of bands B and C is Mg^{2+} dose dependent. In the presence of 5 mM Mg^{2+}, the amount of band A increases to 4%, while the amounts of B and C decrease to 4% and 5%, respectively, compared to that of no Mg^{2+}. Interestingly, the presence of 20 or 50 mM Mg^{2+} leads to a trypsin digestion pattern that is different from that of 0 or 5 mM Mg^{2+}. At 50 mM Mg^{2+},

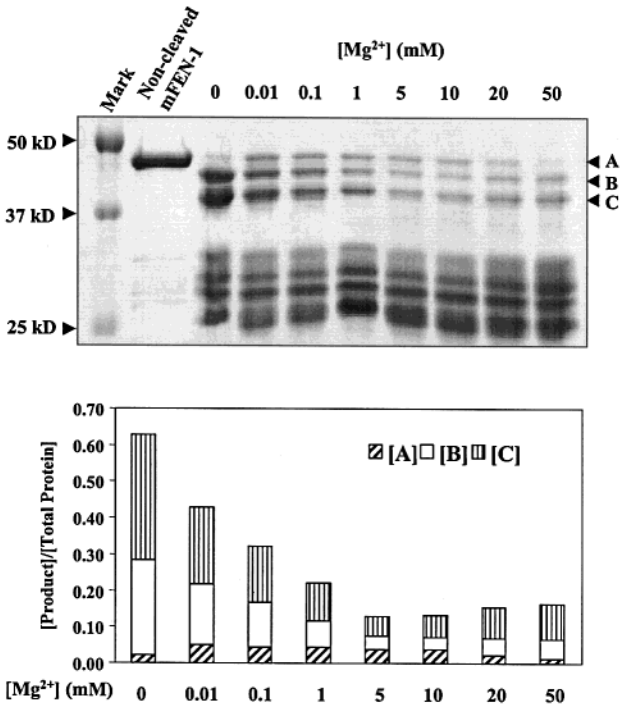

FIGURE 3: Effects of Mg^{2+} concentration on the trypsin digestion pattern of mFEN-1. The trypsin sensitivity assay was carried out by mixing 80 ng of sequencing-grade trypsin and 80 μg of purified mFEN-1 dissolved in 50 mM Tris-HCl (pH 8.0) buffer containing the indicated amounts of Mg^{2+}. Lane 1 is the standard proteins with known molecular masses. Lane 2 shows one-third input of mFEN-1 without treatment of trypsin, and lanes 3−10 are mFEN-1 treated with trypsin in the presence of 0, 0.01, 0.1, 1, 5, 10, 20, or 50 mM Mg^{2+}, correspondingly. The reactions were incubated at 25 °C for 1 h, and the digestion products were analyzed by 4%−20% gradient SDS−PAGE (Bio-Rad, Hercules, CA). The arrows indicate the positions of three digestion products, A, B, and C. The intensities of the single band (noncleaved mFEN-1) in lane 2 and bands A, B, and C in each of lanes 3−10 were quantified using the IPLab Gel program, and the ratios of [A], [B], and [C] over [noncleaved mFEN-1] were calculated and shown in the bottom panel.

intensities of bands B and C change to 5% and 10%, correspondingly, and the intensity of band A changes to 1% (Figure 3). The pattern of Mg^{2+} concentration-dependent conformational changes correlates to the pattern of Mg^{2+} concentration-dependent nuclease activity (Figure 2). Control reactions were performed in the same conditions except that BSA was used as the substrate for trypsin digestion. The results showed that the concentration of Mg^{2+} has no effect on the trypsin digestion pattern of BSA (data not shown).

Varying Concentrations of Mg^{2+} Alter the DNA Substrate Binding Capability of mFEN-1. Kinetic data reveal that K_m significantly changes as Mg^{2+} concentration is altered. This suggests that Mg^{2+} modulates enzyme activities through the DNA substrate binding capability of mFEN-1. To further test this hypothesis, the effect of Mg^{2+} concentration on the interaction of mFEN-1 with DNA substrate was investigated. The binding of DNA substrate by mFEN-1 is Mg^{2+} concentration dependent (Figure 4). In the absence of Mg^{2+}, the amount of DNA-bound mFEN-1 is diminished. Five millimolar Mg^{2+} greatly enhances the recruitment of mFEN-1 to the DNA substrate. However, in the presence of 20 or 50 mM Mg^{2+} the formation of the DNA/mFEN-1 complex is decreased.

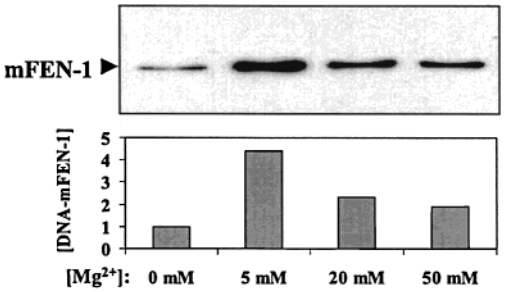

FIGURE 4: Mg^{2+} concentration dependence of DNA substrate binding by mFEN-1. The substrate binding by mFEN-1 in the absence or presence of varying amounts of Mg^{2+} ion was evaluated using a previously published protocol (*45*). Biotinylated DNA substrates were immobilized onto the Neutro-avidin agarose beads and incubated with 10 pmol of purified mFEN-1 in the presence of 0, 5, 20, or 50 mM Mg^{2+}. The proteins bound to agarose beads were analyzed by SDS−PAGE followed by immunoblot using monoclonal anti-FEN-1 antibody. The upper panel shows the results of the substrate binding assay, and the lower panel is the relative amount of protein bound to the DNA substrate. The protein bound to the DNA substrate in the absence of Mg^{2+} is arbitrarily set as 1.

Thermodynamics of Metal Binding by mFEN-1. Thermodynamic properties of metal ion binding to mFEN-1 were determined by ITC experiments. Initial attempts to determine the Mg^{2+} binding constants for mFEN-1 failed because heat changes in response to Mg^{2+} binding are too small to be measured accurately (data not shown). The titration of Mn^{2+} binding by mFEN-1 indicated that two Mn^{2+} ions bound to the protein simultaneously (Figure 5). Two metal ions bind to the enzyme with the same affinity of 2 ± 0.28 μM. Binding of 1 mol of Mn^{2+} to mFEN-1 releases 0.97 ± 0.019 kcal of heat. The metal binding to mFEN-1 leads to a positive entropy change of 22.72 cal/(mol·deg).

Two Mg^{2+} Binding Sites in the Active Center Have Distinct Roles in Modulation of the Substrate Binding Capability and the Protein Conformation of mFEN-1. The active center of mFEN-1 possesses two Mg^{2+} binding sites which also bind Mn^{2+}. It is not known whether these two sites play different roles in activation of the enzyme. To answer this question, a combination of mutagenesis, metal binding measurement, activity assay, trypsin sensitivity assay, and the substrate binding assay was employed. According to the previous crystal structure of aFEN-1 and the three-dimensional model structure of mFEN-1, it was suggested that D86 directly coordinated with the first metal (M1), while D181 coordinated with the second metal (M2) (*26*; Figure 6A). Two mutants, D86A and D181A, were generated as His-tagged fusion proteins. The conformations of mFEN-1 and the two mutants were analyzed by circular dichroism (CD) spectroscopy, and no spectral differences were observed among these three proteins (data not shown). The activity assay revealed that both D86A and D181A cleaved neither flap-specific nor nick-specific DNA substrate (data not shown). To demonstrate that D86A and D181A bind only one metal ion per enzyme molecule as suggested by the model structure, ITC experiments on D86A and D181A were conducted under the same condition as for the wild-type enzyme. However, both mutant proteins precipitated during the titration. By the alternative ultrafiltration method, the wild-type mFEN-1 was shown to bind 2.3 and 2.1 Mg^{2+} ions per enzyme molecule at protein concentrations of 173 and 331 μM, respectively, in agreement with the ITC data (Table 3 and Figure 5). D86A

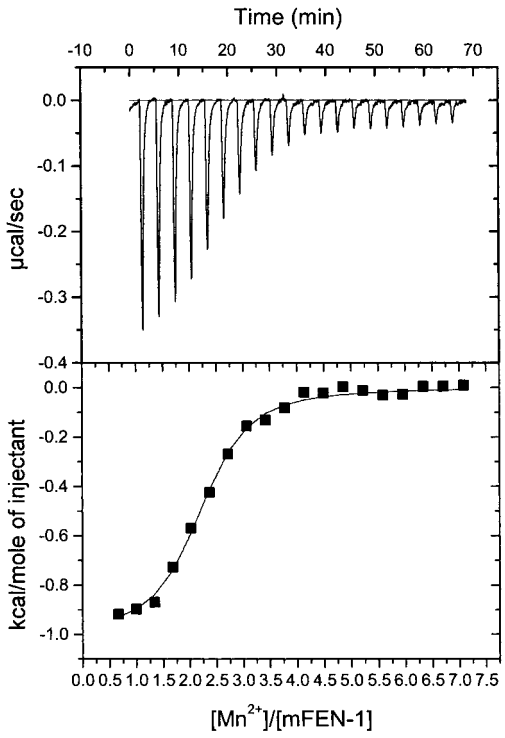

FIGURE 5: Isothermal calorimetric titration of Mn^{2+} with mFEN-1. mFEN-1 was suspended in 50 mM Tris-HCl, pH 7.5. A 250 μL syringe loaded with 2 mM $MnCl_2$ solution provided a series of automatic injections of 10 μL each into the protein solution. The heat changes were recorded at 23.5 °C for each injection (upper panel). Identical injections were carried out using a solution without protein in the sample cell. In this case, the heat of dilution was measured for each injection (data not shown) and subtracted from the respective data obtained with the mFEN-1 sample to determine heat changes due solely to Mn^{2+} binding. These results are shown in the bottom panel. The line drawn through the data points represents nonlinear least-squares fits.

binds 1.0 and 1.2 Mg^{2+} ions at protein concentrations of 221 and 439 μM, correspondingly. D181A binds 0.9 and 1.3 Mg^{2+} ions at protein concentrations of 206 and 417 μM, respectively (Table 3). Both of the mutants can bind only one metal ion. These data indicate that the wild-type mFEN-1 binds two Mg^{2+} ions, while the mutant proteins lose one metal binding site.

Trypsin sensitivity assay indicated that, in the presence of 5 mM Mg^{2+}, D86A showed conformational changes similar to those of the wild-type enzyme, but D181A showed no conformational changes in response to Mg^{2+} binding (Figure 7). In the presence of 50 mM Mg^{2+}, all three proteins displayed similar trypsin digestion patterns. The DNA substrate binding assay showed that, compared with wild-type mFEN-1, D181A has good substrate binding ability, but the substrate binding ability of D86A is hindered (Figure 8). In the DNA binding assay, due to the slow hydrolysis of DNA by mFEN-1, less wild-type enzyme bound to the DNA−agarose beads than D181A.

DISCUSSION

FEN-1 requires Mg^{2+} for cleavage of its DNA substrates with unique or abnormal structures during DNA replication and repair processes. Understanding the roles of divalent metal ions in the regulation of mFEN-1 activities is crucial for elucidating structure−function relationships for this group

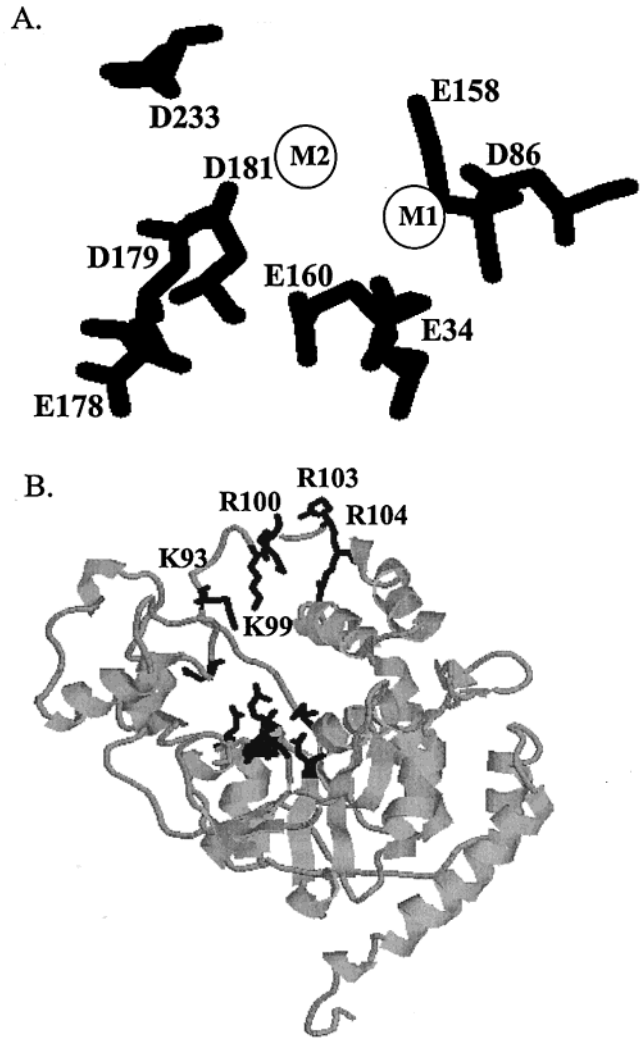

FIGURE 6: Three-dimensional structural model of mFEN-1. The model structure was created by the Swiss-model program (*48*−*50*) using the crystal structure of the *P. furious* FEN-1 homologue as the template. The model structure of mFEN-1 was viewed and manipulated by the Rasmol program (University of Massachusetts, Amherst, MA). (A) Proposed Mg^{2+} binding sites in the active center. The ion binding sites were predicted on the basis of previous studies (*23*, *26*). Only residues that are involved in the interaction with the cation ion were displayed. (B) Structural model of mFEN-1. The positively charged residues in the loop region were marked and labeled. The side chains of these residues in the loop region and the negatively charged residues in the active center were displayed.

Table 3: Stoichiometry of Mg^{2+} Binding by mFEN-1 and Its Mutants Determined by Ultrafiltration

mFEN-1	protein concn (μM)	Mg^{2+} no. exptl	Mg^{2+} no. predicted
wild type	173	2.3 ± 0.1	2
	331	2.1 ± 0.09	
D86A	221	1.0 ± 0.06	1
	449	1.2 ± 0.07	
D181A	206	0.9 ± 0.1	1
	417	1.3 ± 0.2	

of structure-specific nucleases. While the essential amino acid residues that coordinate Mg^{2+} have been identified and Mg^{2+}-induced conformational changes have also been observed, the mechanism by which the metal ions regulate the enzyme activity has not been delineated. Detailed kinetic and

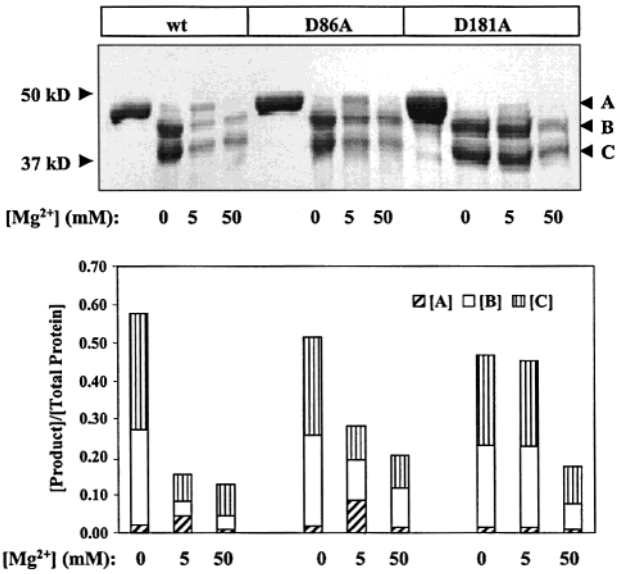

FIGURE 7: $[Mg^{2+}]$ dependence of conformational changes of mFEN-1, D86A, and D181A. The $[Mg^{2+}]$-dependent conformational changes of mFEN-1 and its mutants were monitored by trypsin sensitivity assay. The trypsin digestion products of mFEN-1 proteins in the presence of the indicated amount of Mg^{2+} ions were analyzed by 4%−20% gradient SDS−PAGE. The arrows indicate the positions of three digestion products, A, B, and C. Lanes 1, 5, and 9 are one-third input of noncleaved wt mFEN-1, D86A, and D181A, respectively. Lanes 2−4 are mFEN-1 treated with trypsin at 0, 5, and 50 mM Mg^{2+}, respectively. Lanes 6−8 are D86A cleaved by trypsin at 0, 5, and 50 mM Mg^{2+}, correspondingly, and lanes 10−12 are D181A digested by trypsin at 0, 5, and 50 mM Mg^{2+}, respectively. The intensities of noncleaved proteins in lane 1, 5, or 9 and bands A, B, and C in lanes 3−10 were quantified using the IPLab Gel program. The ratios of [A], [B], and [C] over the corresponding [noncleaved protein] were calculated and shown in the bottom panel.

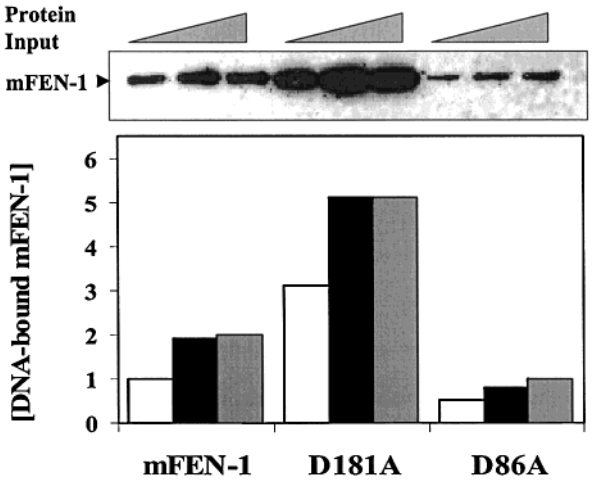

FIGURE 8: $[Mg^{2+}]$ dependence of DNA substrate binding by mFEN-1, D86A, and D181A. Flap DNA substrate bound Neutro-avidin agarose was mixed with 5, 10, or 20 pmol of purified mFEN-1, D86A, or D181A in a buffer solution containing 30 mM Hepes−NaOH, pH 7.5, 125 mM NaCl, 0.2 mg/mL BSA, 1 mM dithiothreitol (DTT), and 5 mM $MgCl_2$. DNA-bound proteins were resolved in 10% SDS−PAGE and detected by immunoblot using monoclonal anti-FEN-1 antibody (upper panel). The relative amounts of DNA-bound proteins were quantified by the IPLab Gel program (bottom panel). The DNA-bound wild-type mFEN-1 is arbitrarily set as 1.

thermodynamic analyses of metal ion effects on enzyme activity, substrate binding, and protein conformation per-

formed in this study enable us to propose distinct roles for multiple divalent metal ion binding sites.

Mg^{2+}-induced conformational changes of hFEN-1 were first observed using the small-angle X-ray diffraction technique and Fourier transform infrared spectroscopy (FTIR; *39*, *40*). Although no major conformational changes occur at the secondary structure level upon Mg^{2+} binding, as monitored by CD spectroscopy of mFEN-1 at different concentrations of Mg^{2+} (data not shown), limited trypsin digestion experiments reveal conformational changes. The pattern of conformational changes thus deduced corresponds to the pattern of Mg^{2+} concentration-dependent enzyme activities of mFEN-1 (Figures 2 and 3). This suggests that the conformational changes are essential for stimulation of the enzyme. The trypsin sensitivity assay also provides information on accessibility of positively charged amino acid residues, which are critical in DNA binding and cleavage. mFEN-1 is a protein rich in Lys and Arg residues with 10 basic residues (R29, R47, R70, R73, K80, K93, K99, R100, R103, and R104) that are conserved in eukaryotic FEN-1 (*24*). Particularly, R47 and R70 were identified to be essential for substrate binding (*28*). K93, K99, R100, R103, and R104, which are located in the loop region (Figure 6B), were first proposed to interact with the single-stranded DNA of the flap-specific DNA substrate (*26*). Recent mutagenesis studies showed that the site-directed mutant R100A completely loses not only flap endonuclease but also exonuclease activities, while the R103A/R104A mutant displays a partial loss in both activities (Qiu et al., unpublished data), thus suggesting that these residues are critical for catalysis. Normally, positively charged residues in the loop region are expected to be located on the surface of the protein and to be accessible for trypsin cleavage. Limited digestion of mFEN-1 (43 kDa) by trypsin in the absence of Mg^{2+} produces two major fragments with molecular masses of 40 kDa (band B) and 39 kDa (band C, Figure 3). This indicates that side chains of K93, K99, R100, R103, and R104, which may form salt bridges with acidic residues in the active center, are hidden inside the protein and not easily accessible to trypsin. In the presence of millimolar levels of Mg^{2+}, the amounts of products B and C decrease to very low levels (Figure 3). This suggests that incorporation of Mg^{2+} into the active center induces conformational changes in mFEN-1, leading to possible breakage of salt bridges and exposure of basic residues in the loop region.

The other consequence of Mg^{2+} binding by mFEN-1 is the enhancement of DNA substrate binding ability of the enzyme. Studies on hFEN-1 showed that mutation in the metal ion binding site resulted in a decrease of DNA substrate binding ability (*47*). In this study, the Mg^{2+} concentration effect on substrate binding efficacy of mFEN-1 was directly evaluated using both the kinetic analysis and the DNA substrate binding assay. Data from both experiments consistently showed that the physiological concentration of Mg^{2+}, which is at millimolar levels (*32*), stimulates mFEN-1 to bind DNA substrate.

Mg^{2+} is essential for mFEN-1 activities; however, when the metal ion levels are higher than 20 mM, enzyme activities are inhibited. This inhibition may result from protein conformational changes or decrease of DNA binding ability as a result of nonspecific binding of the cation by the enzyme or by a general electrostatic effect. Our data revealed that, in the presence of high concentrations of Mg^{2+} ions (>20 mM), the protein was induced to a different conformation. As monitored by the trypsin sensitivity assay, in the presence of 20 or 50 mM Mg^{2+}, the accumulation of product A decreased and the accumulation of products B and C slightly increased, compared to those at 5 mM Mg^{2+} (Figure 3). High levels of Mg^{2+} also inhibited substrate binding as shown by direct steady-state kinetic analysis and substrate binding assay. High levels of Mg^{2+} may disrupt the specific interaction between mFEN-1 and DNA substrate. Taken together, it suggests that Mg^{2+} regulates mFEN-1 activities by modulating the protein's conformation and its substrate binding capability.

Two clusters of acidic amino acid residues were identified to be important for catalysis and metal ion binding, suggesting two Mg^{2+} binding sites in the active center (*23*, *47*). In this study, use of highly sensitive ITC allowed determination of the stoichiometry of the metal ion binding and the thermodynamic parameters, binding affinity (K_d) and enthalpy change (ΔH). While both the ITC and ultrafiltration data showed that two metal ions bound to mFEN-1, we could not rule out further metal ions incorporating into the enzyme in the presence of high metal concentrations, at which the enzyme activities are inhibited. Neither could we rule out that metal ions further incorporate into the enzyme in the presence of DNA substrate. According to the thermodynamic data, the two Mn^{2+} ions bind to the enzyme at the same time with an apparent affinity of 2 μM. Although we could not determine accurate Mg^{2+} binding affinity due to practical problems, we could estimate that the apparent affinity of Mg^{2+} binding by mFEN-1 is at micromolar or submillimolar levels, according to the Mg^{2+} concentration-dependent activity assay and Mg^{2+} concentration-dependent conformational changes (Figures 2 and 3). Since the free Mg^{2+} concentration in vivo is at millimolar levels (*32*), the mFEN-1 is likely to exist as a metalloenzyme under physiological conditions. While the two metal ion binding sites in the active center have the same binding affinity, their roles in the regulation of enzyme activity are distinct. Mutant D86A, with a defect in the M1 metal ion binding site (Figure 6A), has a decreased substrate binding ability, but, like the wild-type enzyme, it undergoes Mg^{2+}-induced conformational changes. On the other hand, mutant D181A, with a defect in the M2 metal ion binding site (Figure 6A), shows no conformational changes in response to Mg^{2+} binding, but it binds substrate as efficiently as does the wild-type enzyme. Thus, it is deduced that binding of Mg^{2+} to the M1 site of mFEN-1 is required for substrate binding, binding of the cation to the M2 site is essential for productive conformational changes of mFEN-1, and both are required for stimulation of the enzyme activities. Additional metal ions, which weakly interact with the protein when Mg^{2+} concentration is higher than 20 mM, inhibit substrate binding, thus suppressing the enzymatic activity.

ACKNOWLEDGMENT

We thank Dr. Michal Zolkiewski for the generous use of the isothermal titration calorimeter and for technical assistance, Dr. Junzhuan Qiu for sharing unpublished data and stimulating discussions, and Qing Chai, Philis Wu, Steve

Alas, and other members in the Shen laboratory for technical support and critical reading of the manuscript.

REFERENCES

1. Harrington, J. J., and Lieber, M. R. (1994) *EMBO J. 13*, 1235−1246.
2. Waga, S., and Stillman, B. (1994) *Nature 369*, 207−212.
3. Waga, S., Bauer, G., and Stillman, B. (1994) *J. Biol. Chem. 269*, 10923−10934.
4. Harrington, J. J., and Lieber, M. R. (1994) *Genes Dev. 8*, 1344−1355.
5. Turchi, J. J., Huang, L., Murante, R. S., Kim, Y., and Bambara, R. A. (1994) *Proc. Natl. Acad. Sci. U.S.A. 91*, 8903−9807.
6. Murray, J. M., Tavassoli, M., al Harithy, R., Sheldrick, K. S., Lehmann, A. R., Carr, A. M., and Watts, F. Z. (1994) *Mol. Cell. Biol. 14*, 4878−4888.
7. Reagan, M. S., Pittenberger, C., Siede, W., and Friedberg, E. C. (1995) *J. Bacteriol. 177*, 364−371.
8. Sommers, C. H., Miller, E. J., Dujon, B., Prakash, S., and Prakash, L. (1995) *J. Biol. Chem. 270*, 4193−4196.
9. Johnson, R. E., Kovvali, G. K., Prakash, L., and Prakash, S. (1995) *Science 269*, 238−240.
10. Tishkoff, D. X., Filosi, N., Gaida, G. M., and Kolodner, R. D. (1997) *Cell 88*, 263−263.
11. Yoon, J.-H., Swiderski, P., Kaplan, B. E., Takao, M., Yasui, A., Shen, B., and Pfeifer, G. P. (1999) *Biochemistry 38*, 4809−4817.
12. Brosh, R. M., Jr., Kobbe, C., Sommers, J. A., Karmaker, P., Opresko, P. L., Piotrowski, J., Dianova, I., Dianov, G., L., and Bohr, V. A. (2001) *EMBO J. 20*, 5791−5801.
13. Li, X., Li, J., Harrington, J. J., Lieber, M. R., and Burgers, P. M. J. (1995) *J. Biol. Chem. 270*, 22109−22112.
14. Wu, X., Li, J., Li, X., Hsieh, C.-L., Burgers, P. M. J., and Lieber, M. R. (1996) *Nucleic Acids Res. 24*, 2036−2043.
15. Qiu, J., Li, X., Frank, G., and Shen, B. (2001) *J. Biol. Chem. 276*, 4901−4908.
16. Gordenin, D. A., Kunkel, T. A., and Resnick, M. A. (1997) *Nat. Genet. 16*, 116−118.
17. Freudenreich, C. H., Kantrow, S. M., and Zakian, V. A. (1998) *Science 279*, 853−856.
18. Spiro, C., Pelletier, R., Rolfsmeier, M. L., Dixon, M. J., Lahue, R. S., Gupta, G., Park, M. S., Chen, X., Mariappan, S. V. S., and McMurray, C. T. (1999) *Mol. Cell 4*, 1079−1085.
19. Tom, S., Henricksen, L. A., and Bambara, R. A. (2000) *J. Biol. Chem. 275*, 10498−10505.
20. Negritto, M. C., Qiu, J., Ratay, D. O., Shen, B., and Bailis, A. M. (2001) *Mol. Cell. Biol. 21*, 2349−2358.
21. Murante, R., Rust, L., and Bambara, R. A. (1995) *J. Biol. Chem. 270*, 30377−30383.
22. Bambara, R. A., Murante, R. S., and Henricksen, L. A. (1997) *J. Biol. Chem. 272*, 4647−4650.
23. Shen, B., Nolan, J. P., Sklar, L. A., and Park, M. S. (1996) *J. Biol. Chem. 271*, 9173−9176.
24. Shen, B., Qiu, J., Hosfield, D., and Tainer, J. A. (1998) *Trends Biochem. Sci. 23*, 171−173.
25. Ceska, T. A., Sayers, J. R., Stier, G., and Suck, D. (1996) *Nature 382*, 90−93.
26. Hosfield, D., Mol, C. D., Shen, B., and Tainer, J. A. (1998) *Cell 95*, 135−146.
27. Hwang, K. Y., Baek, K., Kim, H.-Y., and Cho, Y. (1998) *Nat. Struct. Biol. 5*, 707−713.
28. Qiu, J., Bimston, D. N., Partikian, A., and Shen, B. (2002) *J. Biol. Chem. 277*, 24659−24666.
29. Mueser, T. C., Nossal, N. G., and Hyde, C. C. (1996) *Cell 85*, 1101−1112.
30. Shen, B., Nolan, J. P., Skla, L. A., and Park, M. S. (1997) *Nucleic Acids Res. 25*, 3332−3338.
31. Xu, Y., Derbyshire, V., Ng, K., Sun, X. C., Grindley, N. D. F., and Joyce, C. M. (1997) *J. Mol. Biol. 268*, 284−302.
32. Hartwig, A. (2001) *Mutat. Res. 475*, 113−121.
33. Sirover, M. A., and Loeb, L. A. (1977) *J. Biol. Chem. 252*, 3605−3610.
34. Barzilay, G., Mol, C. D., Robson, C. N., Walker, L. J., Cunningham, R. P., Tainer, J. A., and Hickson, I. D. (1995) *Nat. Struct. Biol. 2*, 561−568.
35. O'Donovan, A., and Wood, R. D. (1993) *Nature 363*, 185−188.
36. Welsh, K. M., Lu, A.-L., Clark, S., and Modrich, P. (1987) *J. Biol. Chem. 262*, 15624−15629.
37. Nakamura, H., Oda, Y., Iwai, S., Inoue, H., Ohtsuka, E., Kanaya, S., Kimura, S., Katsuda, C., Katayanagi, K., and Morikawa, K, (1991) *Proc. Natl. Acad. Sci. U.S.A. 88*, 11535−11539.
38. Beese, L., and Steitz, T. A. (1991) *EMBO J. 10*, 25−33.
39. Kim, C., Shen, B., Park, M. S., and Olah, G. A. (1999) *J. Biol. Chem. 274*, 1233−1239.
40. Kim, C. Y., Park, M. S., and Dyer, R. B. (2001) *Biochemistry 40*, 3208−3214.
41. Frank, G., Qiu, J., Zheng, L., and Shen, B. (2001) *J. Biol. Chem. 276*, 36295−36302.
42. Wiseman, T., Williston, S., Brandts, J. F., and Lin, L. (1989) *Anal. Biochem. 179*, 131−137.
43. Lin, K., Mejillano, M., and Yin, H. L. (2000) *J. Biol. Chem. 275*, 27746−27752.
44. Gindler, E. M., and Heth, D. A. (1971) *Clin. Chem. 17*, 662.
45. Gomes, X., and Burgers, P. M. J. (2000) *EMBO J. 19*, 3811−3821.
46. Zhou, T., and Rosen, B. P. (1999) *J. Biol. Chem. 274*, 13854−13858.
47. Frank, G., Qiu, J., Somsouk, M., Weng, Y., Somsouk, L., Nolan, J., and Shen, B. (1998) *J. Biol. Chem. 273*, 33064−33072.
48. Guex, N., and Peitsch, M. C. (1997) *Electrophoresis 18*, 2714−2723.
49. Peitsch, M. C. (1996) *Biochem. Soc. Trans. 24*, 274−279.
50. Peitsch, M. C. (1995) *Bio/Technology 13*, 658−660.

BI025841S